Wendelstein 7-X

IPP Max-Planck-Institut für Plasmaphysik

Error estimation in filament measurements using a synthetic probe

B Shanahan, C Killer, G Pechstein, S A Henneberg, G Fuchert, O Grulke

Plasma Physics and Controlled Fusion **64** 125018 (2021)

IAEA Technical Meeting on Fusion Data Processing, Validation, and Analysis

MAX PLANCK GESELLSCHAFT

EUROfusion

This work has been carried out within the framework of the EUROfusion Consortium and has received funding from the Euratom research and training programme 2014-2018 and 2019-2020 under grant agreement No 633053. The views and opinions expressed herein do not necessarily reflect those of the European Commission.

Plasma filaments

A filament:

- Is a large monopole density perturbation
- Is aligned to the magnetic field (small parallel fluctuations)
- Exhibits a dipole vorticity/potential structure due to a polarizing force.
  Resulting ballistic ExB motion → "blob"

Responsible for significant radial transport in tokamaks

Filament motion determined by:

- The polarizing force
- Currents within the filament
  - Perpendicular filament size
  - Parallel connection length
  - Resistivity
- Magnetic shear

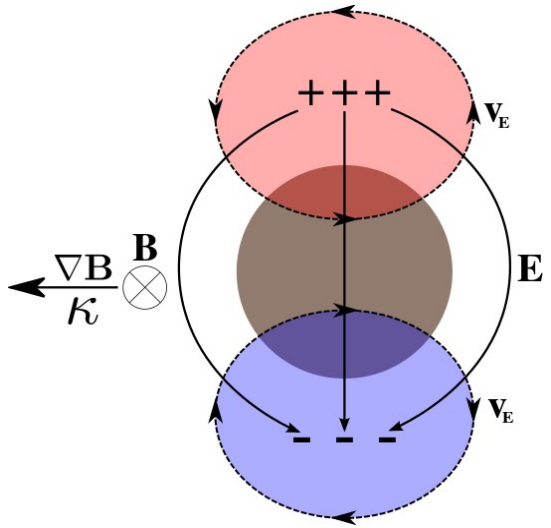

Schematic of a filament

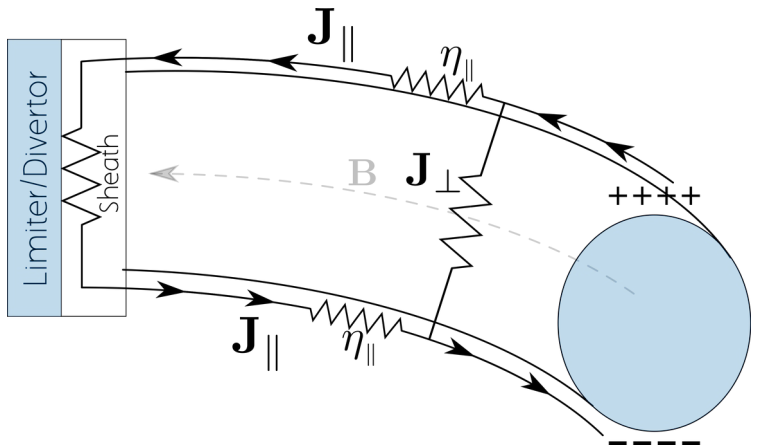

Filament equivalent circuit

[1] D A D'Ippolito et al., *PoP* **18** 6 (2011)

Experimental comparison for W7-X filaments

Filaments have been measured in the W7-X SOL [2]

- Measurements from Multi-Purpose Manipulator probe head
- Knowing this area is free from complicated topology, we compare to drift-plane simulations.
  - *Hermes* model [3] with sheath closures (as simulations are 2D)
- Seeded filaments with initial conditions gleaned from experimental measurements:

$T_0 = 22eV$, $n_0 = 6e18m^{-3}$, $\delta n = 1.3n_0$, $R_0 = 6.1m$

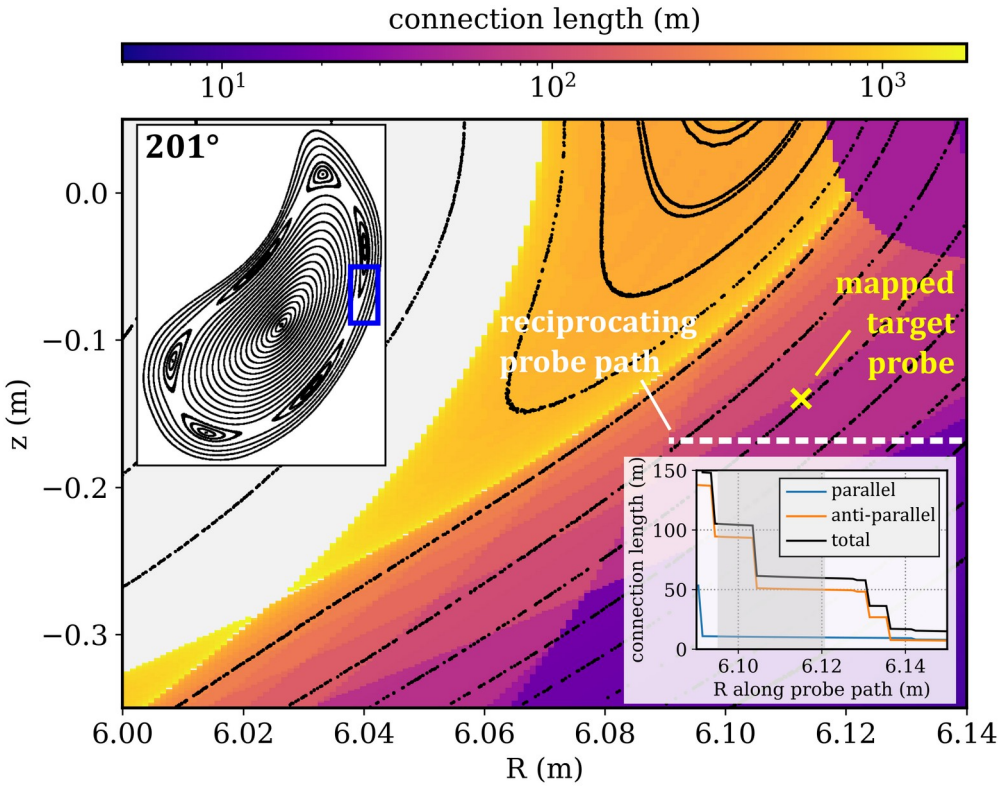

Experimental setup for filament measurements; the reciprocating probe plunges into the plasma (white line) and encounters various connection lengths (color contour)

[3] B Dudson and J Leddy, PPCF **59** 5 (2017)
[2] C Killer, B Shanahan, et al., *PPCF* **62** 085003 (2020)

Experimental comparison for W7-X filaments

Filaments have been measured in the W7-X SOL [2]

- Measurements from Multi-Purpose Manipulator probe head
- Knowing this area is free from complicated topology, we compare to drift-plane simulations.
  - *Hermes* model [3] with sheath closures (as simulations are 2D)
- Seeded filaments with initial conditions gleaned from experimental measurements:

$T_0 = 22eV$, $n_0 = 6e18m^{-3}$, $\delta n = 1.3n_0$, $R_0 = 6.1m$

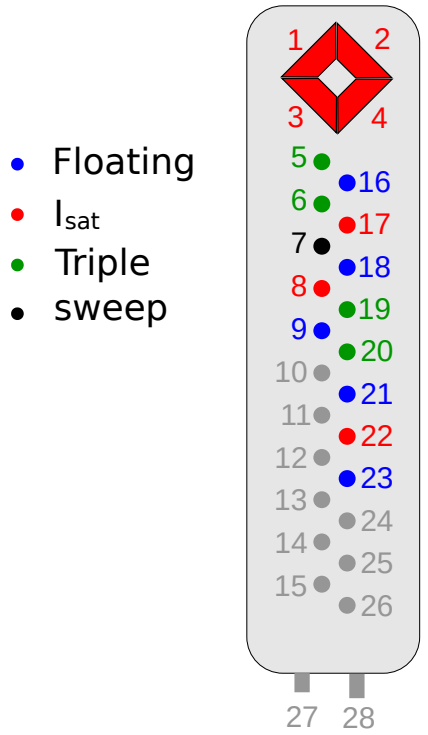

Probe schematic for filament measurements in W7-X. The filament density was determined from I_{sat} probes (red), while radial velocity inferred from neighboring floating potential (blue) probe measurements.

[3] B Dudson and J Leddy, PPCF **59** 5 (2017)
[2] C Killer, B Shanahan, et al., *PPCF* **62** 085003 (2020)

Experimental comparison for W7-X filaments

Filaments have been measured in the W7-X SOL [2]

- Measurements from Multi-Purpose Manipulator probe head
- Knowing this area is free from complicated topology, we compare to drift-plane simulations.
  - *Hermes* model [3] with sheath closures (as simulations are 2D)
- Seeded filaments with initial conditions gleaned from experimental measurements:

  T_0 = 22eV, n_0 = 6e18m^{-3}, $\delta n = 1.3 n_0$, R_0 = 6.1m

$$\frac{\partial n}{\partial t} = -\nabla \cdot (n\mathbf{V}_{E\times B} + n\mathbf{V}_{mag})$$

$$\frac{3}{2}\frac{\partial p_e}{\partial t} = -\nabla \cdot \left(\frac{3}{2}p_e\mathbf{V}_{E\times B} + \frac{5}{2}p_e\mathbf{V}_{mag}\right) - p_e\nabla\cdot\mathbf{V}_{E\times B}$$

$$\frac{\partial \omega}{\partial t} = -\nabla\cdot(\omega\mathbf{V}_{E\times B}) - \nabla\cdot(en\mathbf{V}_{mag}) + \nabla\cdot(\mu_i\nabla_\perp\omega)$$

$$\omega \approx \nabla\cdot\left(\frac{en_0}{\Omega_i B}\nabla_\perp\phi\right)$$

$$\mathbf{V}_{E\times B} = \frac{\mathbf{b}\times\nabla\phi}{B} \qquad \mathbf{V}_{mag} = -\frac{T_e}{e}\nabla\times\frac{\mathbf{b}}{B}$$

[3] B Dudson and J Leddy, PPCF **59** 5 (2017)
[2] C Killer, B Shanahan, et al., *PPCF* **62** 085003 (2020)

Experimental comparison for W7-X filaments

Filaments have been measured in the W7-X SOL [2]

- Measurements from Multi-Purpose Manipulator probe head
- Knowing this area is free from complicated topology, we compare to drift-plane simulations.
  - *Hermes* model [3] with sheath closures (as simulations are 2D)
- Seeded filaments with initial conditions gleaned from experimental measurements:

  T_0 = 22eV, n_0 = 6e18m^{-3}, $\delta n = 1.3 n_0$, R_0 = 6.1m

$$\frac{\partial n}{\partial t} = -\nabla \cdot (n\mathbf{V}_{E\times B} + n\mathbf{V}_{mag})$$

$$\frac{3}{2}\frac{\partial p_e}{\partial t} = -\nabla \cdot \left(\frac{3}{2}p_e\mathbf{V}_{E\times B} + \frac{5}{2}p_e\mathbf{V}_{mag}\right) - p_e \nabla \cdot \mathbf{V}_{E\times B}$$

$$\frac{\partial \omega}{\partial t} = -\nabla \cdot (\omega \mathbf{V}_{E\times B}) - \nabla \cdot (en\mathbf{V}_{mag}) + \nabla \cdot (\mu_i \nabla_\perp \omega)$$

$$\omega \approx \nabla \cdot \left(\frac{en_0}{\Omega_i B}\nabla_\perp \phi\right)$$

$$\mathbf{V}_{E\times B} = \frac{\mathbf{b}\times\nabla\phi}{B} \qquad \mathbf{V}_{mag} = -\frac{T_e}{e}\nabla \times \frac{\mathbf{b}}{B}$$

$$\frac{\partial n}{\partial t} = \ldots - \frac{\sqrt{T_i/m_i}}{2L_\parallel} n$$

$$\frac{\partial p_e}{\partial t} = \ldots - T_e \frac{\sqrt{T_i/m_i}}{2L_\parallel} n$$

$$\frac{\partial \omega}{\partial t} = \ldots + \frac{enc_s}{L_\parallel}\left[1 - \sqrt{\frac{m_i}{4\pi m_e}}\exp(-e\phi/T_e)\right]$$

[3] B Dudson and J Leddy, PPCF **59** 5 (2017)
[2] C Killer, B Shanahan, et al., *PPCF* **62** 085003 (2020)

Experimental comparison for W7-X filaments

Drift plane simulations replicate macroscopic filament transport in W7-X

- Probe cannot distinguish filament shape, and a flat temperature is assumed
  - Shaded regions indicate various filament ellipticities.
  - A temperature perturbation increases velocity
- Filament velocity is slow, due to small ballooning drive (large major radius)
  - Filament transport mostly localized near flux surfaces.

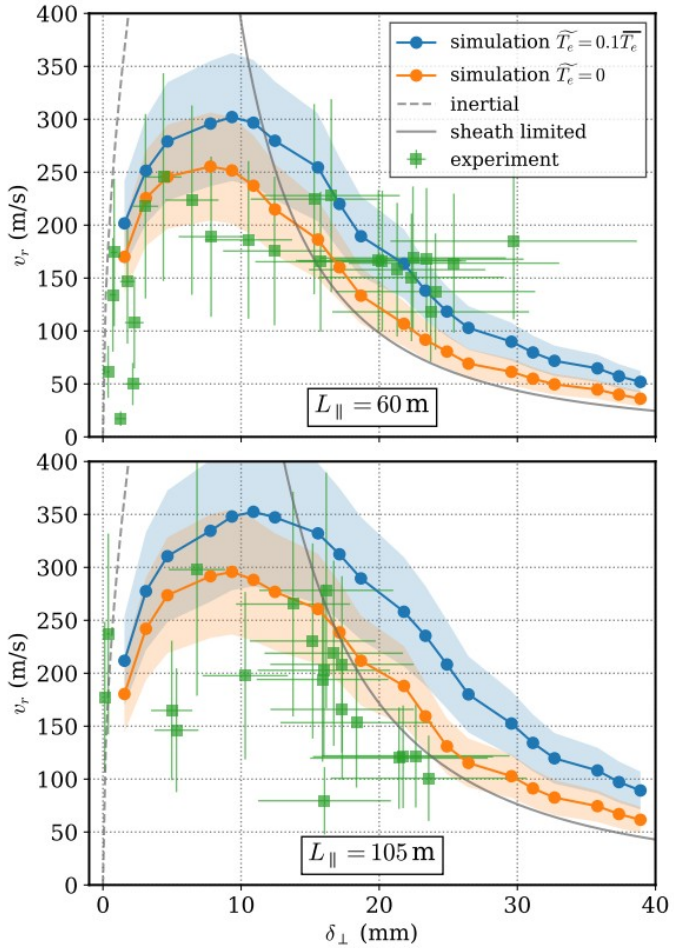

Comparison of measured filament scaling (green) with 2D simulations – both with (blue) and without (orange) a temperature perturbation [2].

[2] C Killer, B Shanahan, et al., *PPCF* **62** 085003 (2020)

Synthetic diagnostic implementation

A synthetic probe has been implemented to mimic conditionally-averaged filament measurements [4]

- Instead of hundreds of conditionally-averaged events at 1 position, average 1 event at hundreds of positions – mimicking many filaments.
  - Triggering mechanism must be changed (instead of 2σ, 1/e of maximum value)
- Singular measurements show potential dipole and density perturbations as the filament passes.
- Temperature perturbations (red) are minimal

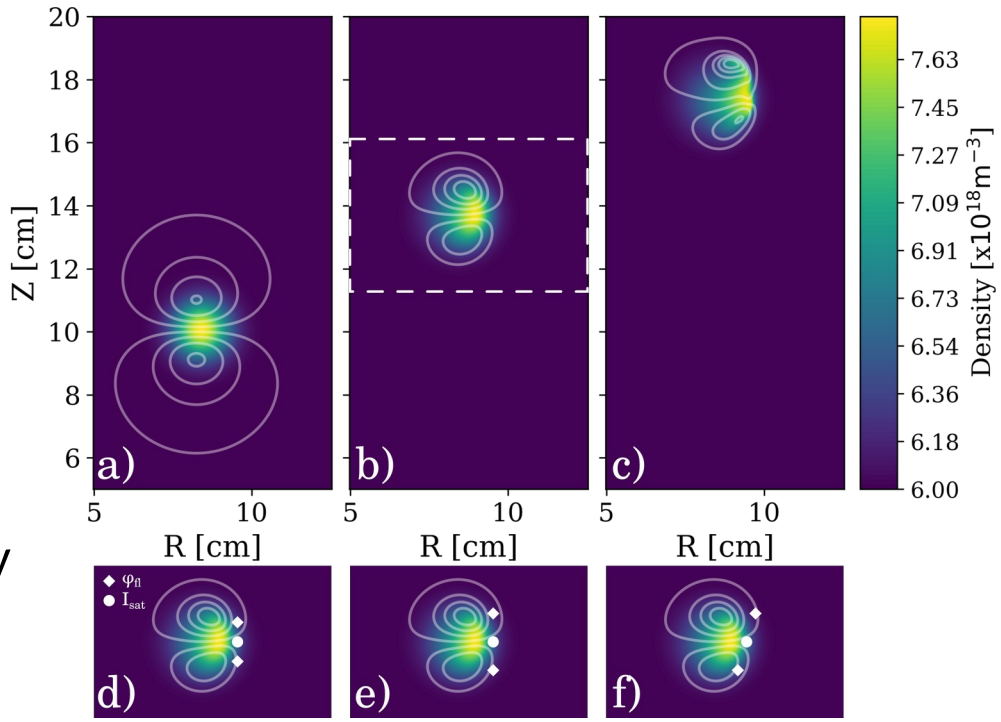

Top: Propagation of a filament in a 2D simulation
Bottom: probe variation relative the to blob; the probes can have varying separation and inclination relative to propagation [4]

[4] B Shanahan et al., *PPCF* **64** 125018 (2021)

Synthetic diagnostic implementation

A synthetic probe has been implemented to mimic conditionally-averaged filament measurements

- Instead of hundreds of conditionally-averaged events at 1 position, average 1 event at hundreds of positions – mimicking many filaments.
  - Triggering mechanism must be changed (instead of 2σ, 1/e of maximum value)
- Singular measurements show potential dipole and density perturbations as the filament passes.
- Temperature perturbations (red) are minimal

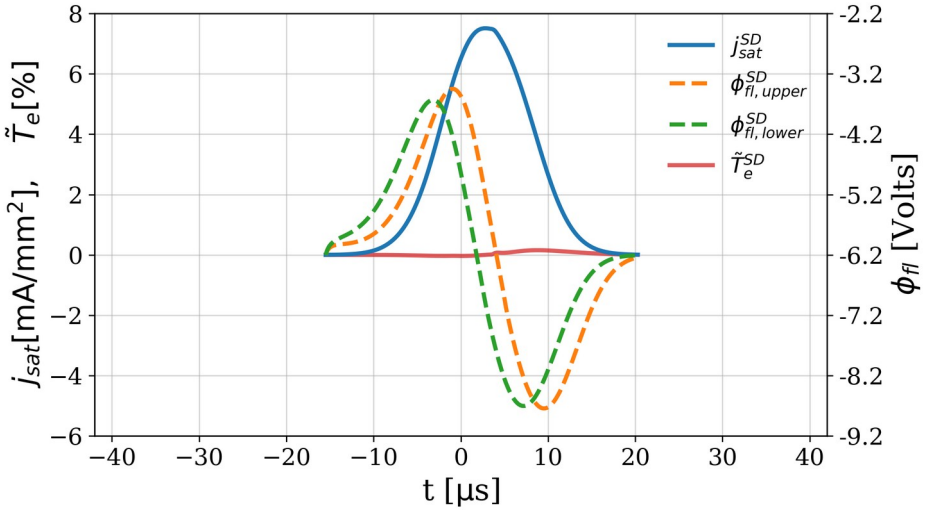

Raw data from the synthetic probe. Ion saturation current density (blue), and floating potential fluctuations (orange, green) as a function of time. Electron temperature fluctuations (red) could potentially shift floating potential measurements.

[4] B Shanahan et al., *PPCF* **64** 125018 (2021)

Synthetic, "conditionally-averaged" measurements

By averaging the measurements at many positions, similar statistics to experiment can be achieved.

- Single measurements (blue) replicate experiment very well
  - Expected, as values are taken from experiment.
- Conditional averaging (green, orange) causes an underestimation of measurements
- Imposing a 100kHz filter (green) as in experiment improves the accuracy
  - Small periphery measurements are removed

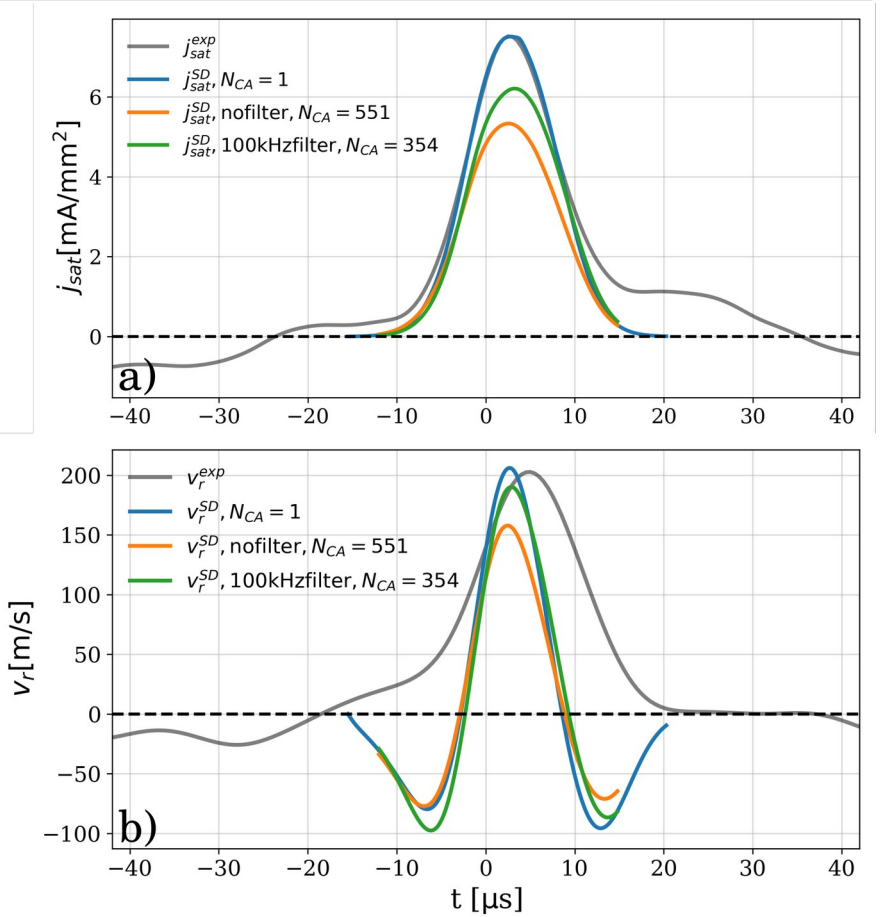

Ion saturation current density (top) and velocity (bottom) measurements from experiment (grey), a single pass of the synthetic probe (blue), and conditionally averaged synthetic measurements with (green) and without (orange) a 100kHz filter

[4] B Shanahan et al., *PPCF* **64** 125018 (2021)

Conceptual picture of underestimation

The CA measurements do not measure the exact diameter of the filament, rather the average distance between two points, δ

- This can be analytically calculated for a circular filament as $\delta = (\pi/4)d \approx 0.79d$
  - As a first assumption, we can assume approximately 20% error.
  - Removing periphery measurements decreases the error

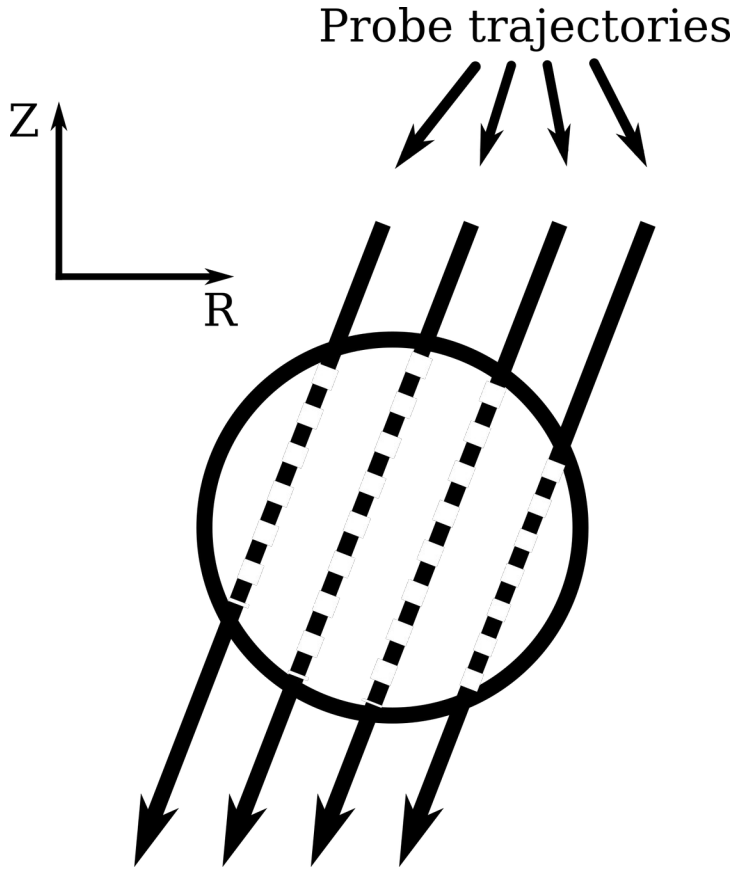

Schematic of probe trajectories through a filament. The average (and measured) distance is smaller than the diameter.

[4] B Shanahan et al., *PPCF* **64** 125018 (2021)

Velocity errors due to probe misalignment

It is not guaranteed that the probe is aligned with the poloidal direction.

- Up to 4° variation between configurations

The error in the velocity measurement is relatively robust to misalignment
(<10% for ±20°)

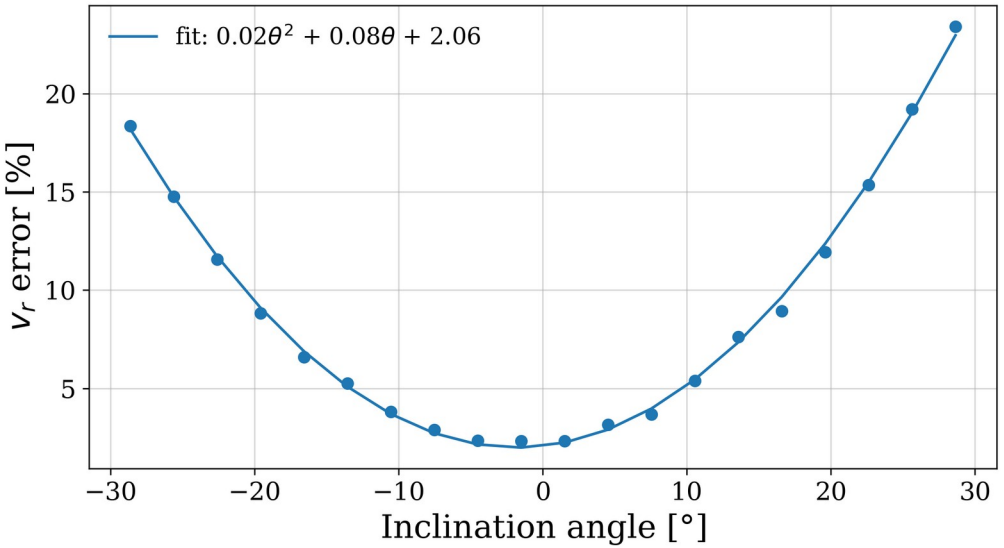

Measured velocity error associated with probe misalignment

[4] B Shanahan et al., *PPCF* **64** 125018 (2021)

Velocity errors due to probe spacing

If the floating potential probes are incorrectly spaced, significant error can be introduced

- Assuming a Gaussian perturbation, the maximum and minimum of the potential dipole should be at $Z_0 \pm \sigma$ and knowing that $\sigma = \delta_\perp/2\sqrt{2}$, we can determine that the ideal pin spacing d is $2\sigma = \delta_\perp/\sqrt{2}$.
- The pin spacing with the lowest associated measurement error d_0 scales indeed as $\delta_\perp/\sqrt{2}$.
- If pins are too close, they can overestimate filament velocity
- Can potentially filter which probes to use based on measured size from the ion saturation current density.

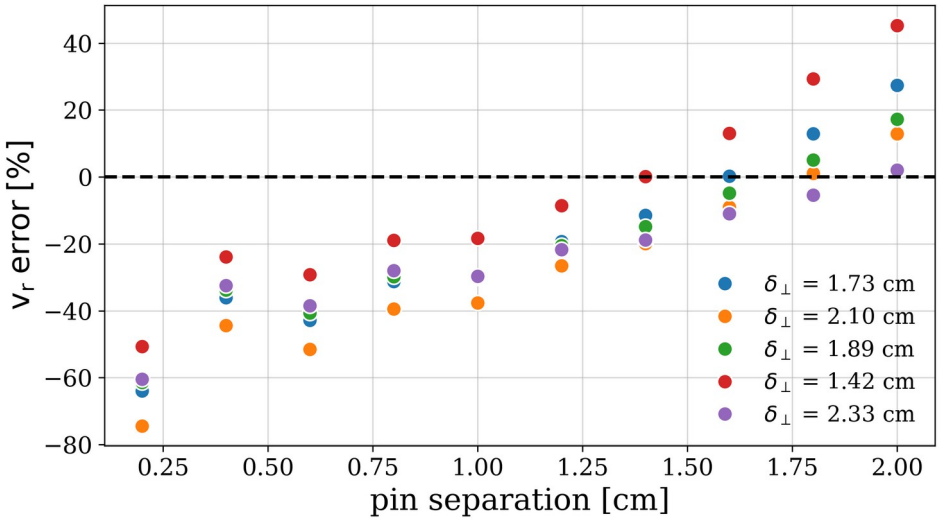

Measured velocity error associated with probe misalignment (top) and pin separation (bottom)

[4] B Shanahan et al., *PPCF* **64** 125018 (2021)

Velocity errors due to probe spacing

If the floating potential probes are incorrectly spaced, significant error can be introduced

- Assuming a Gaussian perturbation, the maximum and minimum of the potential dipole should be at $Z_0 \pm \sigma$ and knowing that $\sigma = \delta_\perp/2\sqrt{2}$, we can determine that the ideal pin spacing d is $2\sigma = \delta_\perp/\sqrt{2}$.
- The pin spacing with the lowest associated measurement error d_0 scales indeed as $\delta_\perp/\sqrt{2}$.
- If pins are too close, they can overestimate filament velocity
- Can potentially filter which probes to use based on measured size from the ion saturation current density.

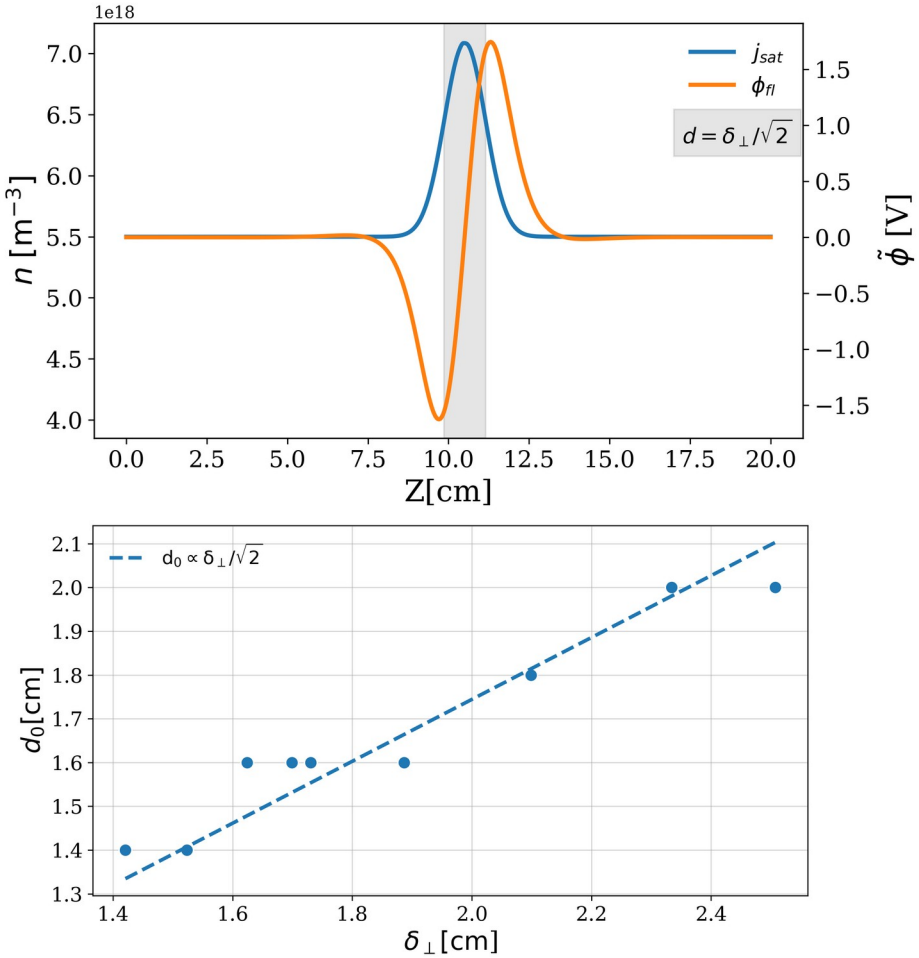

Measured velocity error associated with probe misalignment (top) and pin separation (bottom)

[4] B Shanahan et al., *PPCF* **64** 125018 (2021)

Velocity errors due to probe area

The probes have thus far been considered to have zero-area.

- MPM probes have a poloidal projection of approximately 2mm x 2mm.

Averaging the measurements (both j_{sat} and v_r) over a finite probe area introduces error only for exceptionally large probe areas.

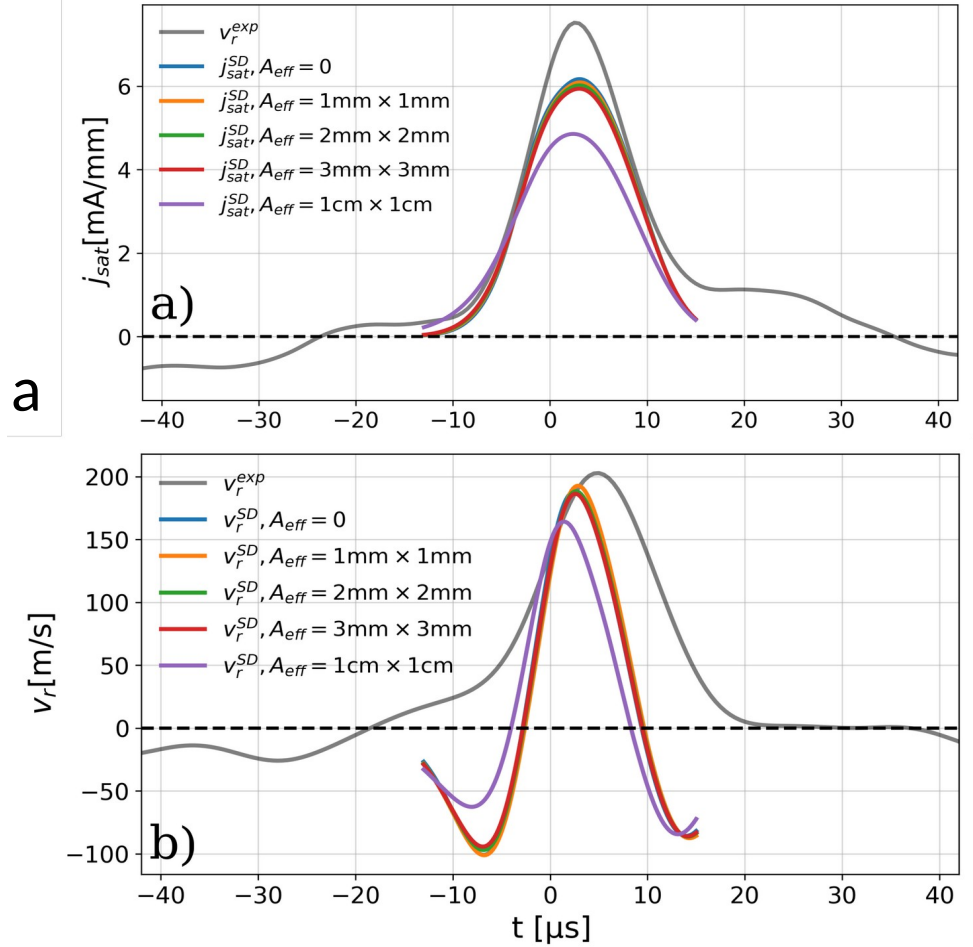

Measured ion saturation current density (top) and radial velocity(bottom) for different probe areas.

[4] B Shanahan et al., *PPCF* **64** 125018 (2021)

Temperature fluctuations affect floating potential

Floating potential measurements are sensitive to temperature:

- $\varphi_{fl} = \varphi_p - 2.8T_e$

Previously, we have assumed flat temperature perturbations, which does not significantly affect measurements

Adding an initial temperature perturbations increases the maximum velocity (due to increasing pressure), but does not significantly affect the velocity measurement.

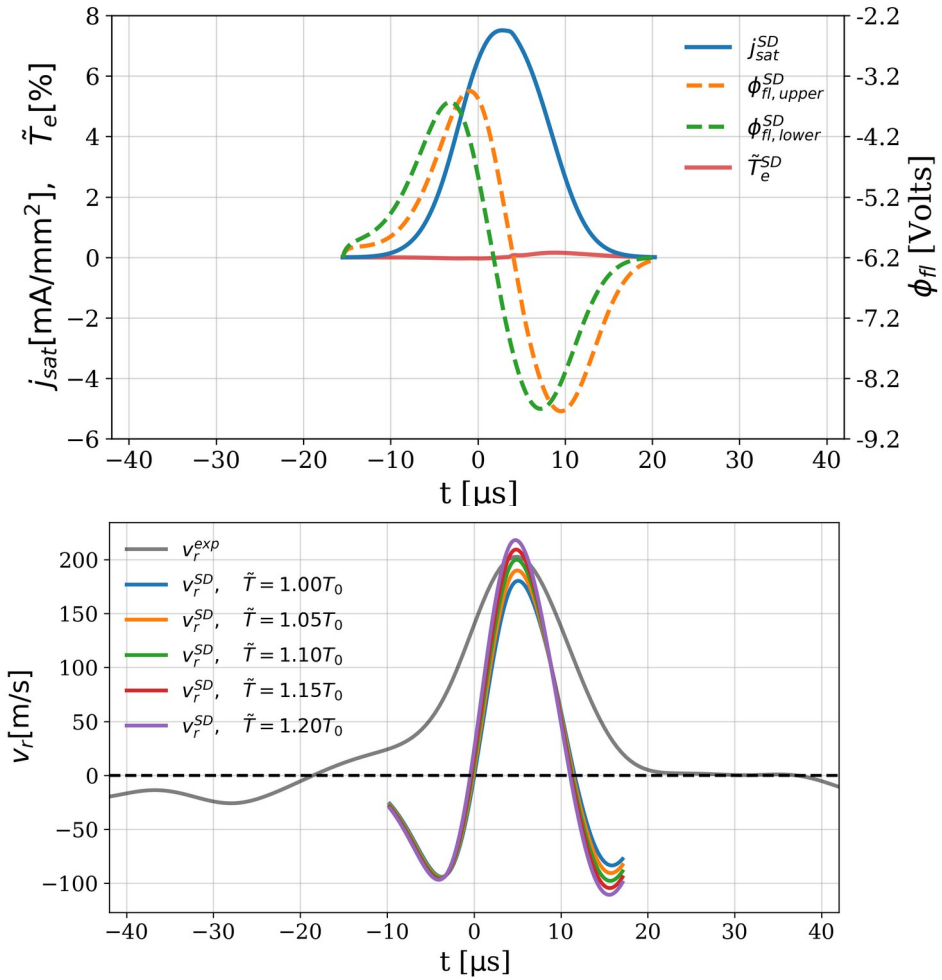

Measured velocity error associated with probe misalignment (top) and pin separation (bottom)

[4] B Shanahan et al., *PPCF* **64** 125018 (2021)

Estimating transport

Contributions of filaments to transport is often estimated as [4]:

- $\Gamma = \langle n v_r \rangle$

However, v_r measurements are sensitive to pin separation

- Significant error introduced if the pin separation does not correspond to the filament size

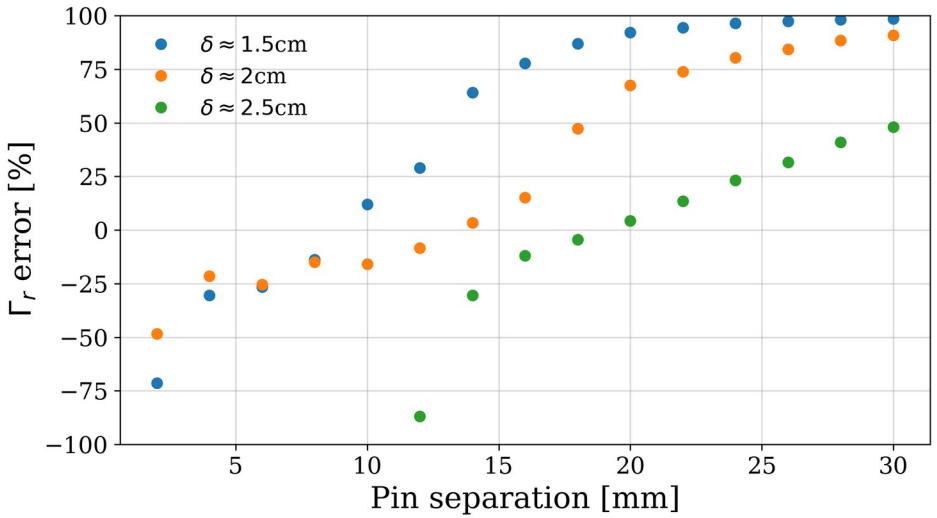

Error in turbulent flux measurements for different filament sizes.

[4] B Shanahan et al., *PPCF* **64** 125018 (2021)
[4] M Endler et al., *NF* **35** 1307 (1995)

A synthetic scaling

To mimic the results from [2], several seeded filament simulations were performed with random initialization (within experimental ranges)

- random initial pressure and perpendicular size
- flat temperature perturbation

Comparison of measured filament scaling

- Filled circles: synthetic probe
- Hollow circles: extracted from simulation
- line: corresponding synthetic and extracted measurements

Larger filaments have more accurately measured velocities, an approximate 20% underestimation of filament size is present.

In general, filaments have an underestimated size and velocity.

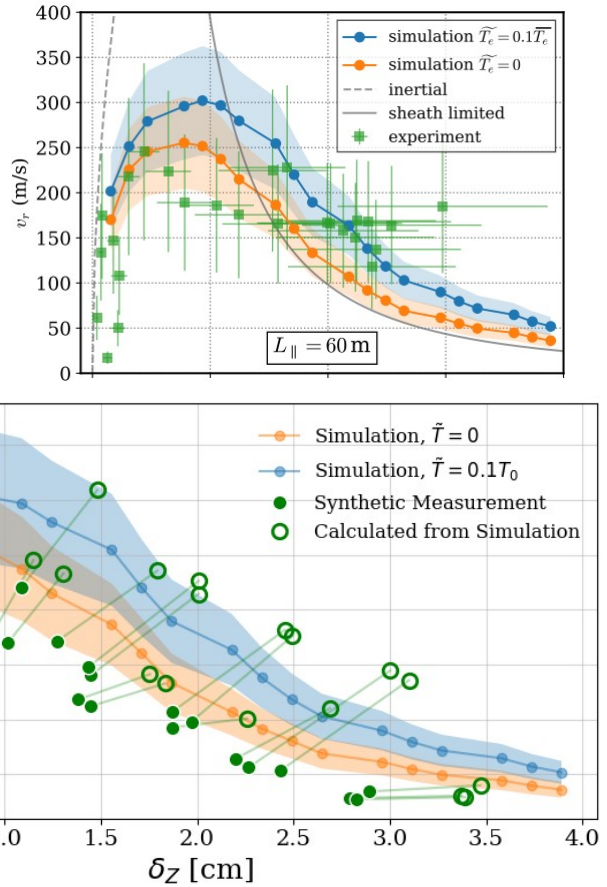

Comparison of filament scaling from a synthetic diagnostic (green filled), directly measured from simulation (green hollow) and the 2D simulations – both with (blue) and without (orange) a temperature perturbation from [2].

[4] B Shanahan et al., *PPCF* **64** 125018 (2021)
[2] C Killer, B Shanahan, et al., *PPCF* **62** 085003 (2020)

Conclusion

A synthetic probe has been developed to explore the errors associated with SOL filament measurements.

In general, an approximate 20% underestimation of filaments is seen

- Primarily introduced by conditionally-averaging grazing measurements

Filament velocity measurements can carry significant error due to probe alignment and spacing

- Fluctuations in temperature and a finite probe area seem not to introduce significant error.

A synthetic scaling has been produced to illustrate shift caused by these errors.

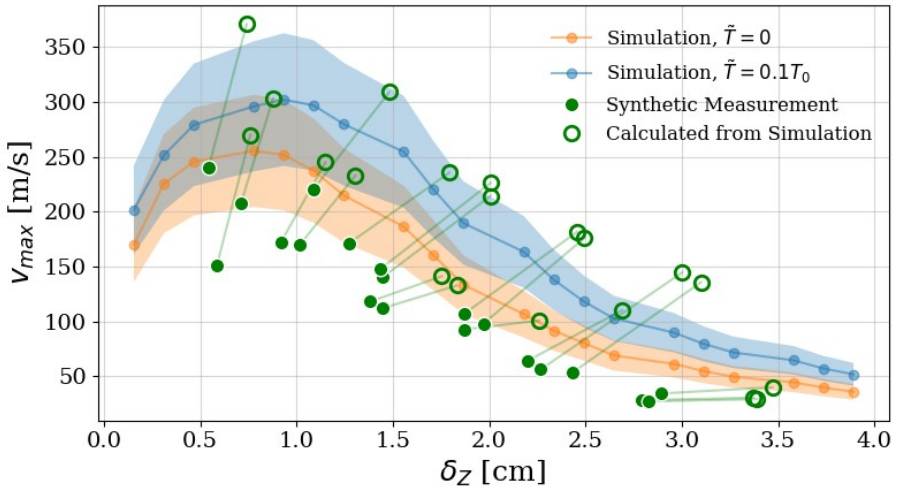

Comparison of filament scaling from a synthetic diagnostic (green filled), directly measured from simulation (green hollow) and the 2D simulations – both with (blue) and without (orange) a temperature perturbation from [2].

[4] B Shanahan et al., *PPCF* **64** 125018 (2021)

Extra Slides

Filament observations in W7-X

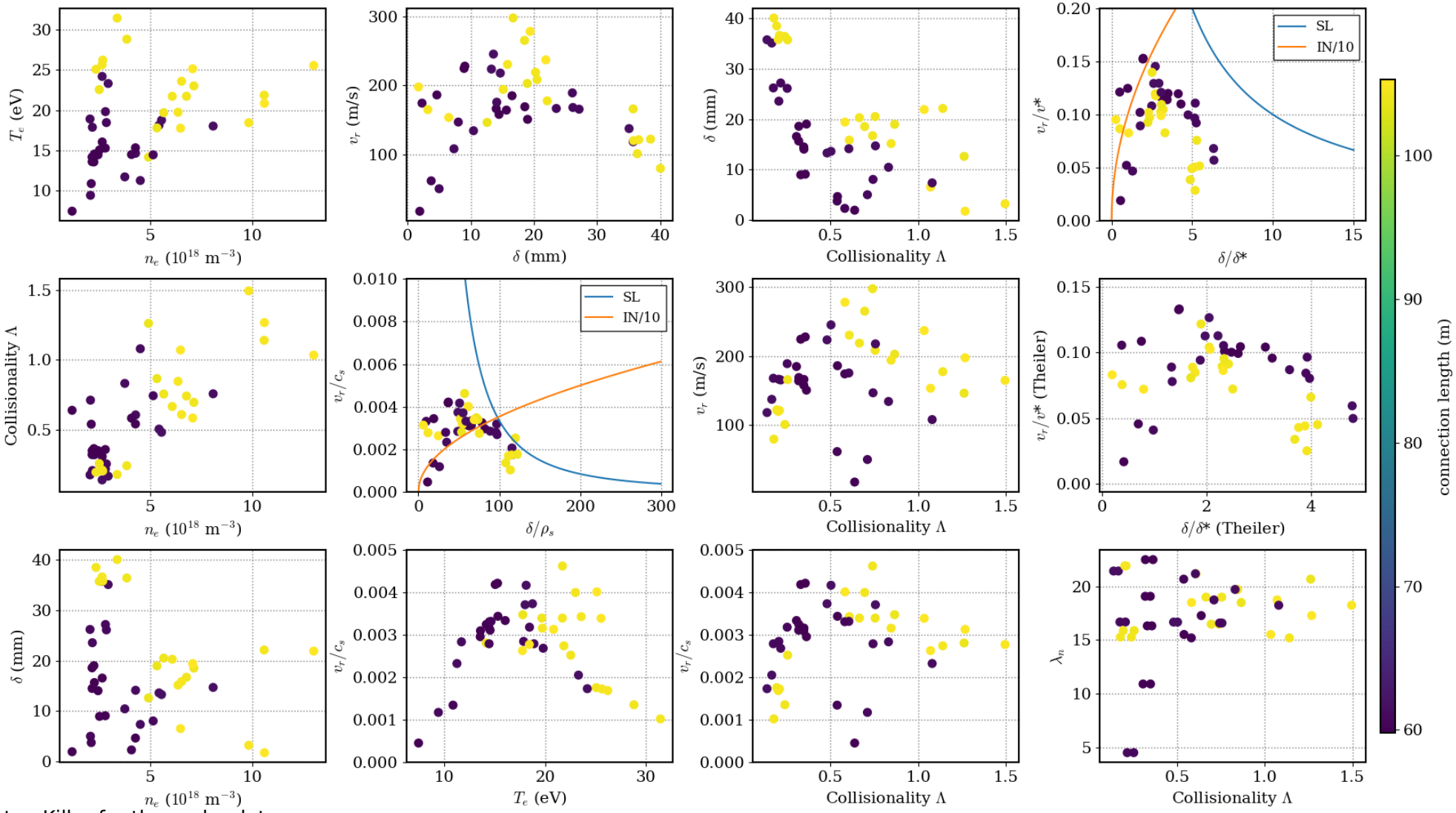

Thanks to Carsten Killer for the probe data

Hermes Equations

$$
\begin{aligned}
\frac{\partial n}{\partial t} &= -\nabla\cdot(n\mathbf{V}_{E\times B} + n\mathbf{V}_{mag}) - \nabla_{||}\left(n_e v_{||e}\right) + \nabla\cdot(D_n\nabla_\perp n) \\
&\quad + S_n - S \\
\frac{3}{2}\frac{\partial p_e}{\partial t} &= -\nabla\cdot\left(\frac{3}{2}p_e\mathbf{V}_{E\times B} + p_e\frac{5}{2}\mathbf{V}_{mag}\right) - p_e\nabla\cdot\mathbf{V}_{E\times B} \\
&\quad -\frac{5}{2}\nabla_{||}\left(p_e v_{||e}\right) + v_{||e}\partial_{||}p_e + \nabla_{||}\left(\kappa_{e||}\partial_{||}T_e\right) \\
&\quad +0.71\nabla_{||}\left(T_e j_{||}\right) - 0.71 j_{||}\partial_{||}T_e + \frac{\nu}{n}j_{||}\left(j_{||} - j_{||0}\right) \\
&\quad +\nabla\cdot\left(\frac{3}{2}D_n T_e\nabla_\perp n\right) + \nabla\cdot(\chi n\nabla_\perp T_e) + S_p - Q \\
\frac{\partial\omega}{\partial t} &= \begin{cases} -\nabla\cdot(\omega\mathbf{V}_{E\times B}) & \text{[Boussinesq]} \\ -\nabla\cdot\left[\frac{1}{2}\left(\omega + \frac{n}{B}\nabla_\perp^2\phi\right)\frac{\mathbf{b}\times\nabla\phi}{B}\right] + \nabla_\perp\cdot\left(\frac{1}{2}\frac{\partial n_i}{\partial t}\frac{1}{B^2}\nabla_\perp\phi\right) \end{cases} \\
&\quad +\nabla_{||}j_{||} - \nabla\cdot(n\mathbf{V}_{mag}) + \nabla\cdot(\mu_i\nabla_\perp\omega) \\
\frac{\partial}{\partial t}\left(n v_{||i}\right) &= -\nabla\cdot\left[n v_{||i}\left(\mathbf{V}_{E\times B} + \mathbf{b}v_{||i}\right)\right] - \partial_{||}p_e \\
&\quad +\nabla\cdot\left(D_n v_{||i}\nabla_\perp n\right) - F \\
\frac{\partial}{\partial t}\left[\frac{m_e}{m_i}\left(v_{||e} - v_{||i}\right) + \frac{1}{2}\beta_e\psi\right] &= \nu j_{||}/n_e + \partial_{||}\phi - \frac{1}{n_e}\partial_{||}p_e - 0.71\partial_{||}T_e \\
&\quad +\frac{m_e}{m_i}\left(\mathbf{V}_{E\times B} + \mathbf{b}v_{||i}\right)\cdot\nabla\left(v_{||i} - v_{||e}\right)
\end{aligned}
$$

2D sheath closures:

$$
\begin{aligned}
\frac{\partial n}{\partial t} &= \ldots - \frac{\sqrt{T_i}}{2L_{||}}n \\
\frac{\partial p_e}{\partial t} &= \ldots - \frac{2}{3}\kappa_{||e}\frac{T_e}{L_{||}} - T_e\frac{\sqrt{T_i}}{2L_{||}}n \\
\frac{\partial\omega}{\partial t} &= \ldots + \frac{1}{L_{||}}n\sqrt{T_e}\left[1 - \sqrt{\frac{m_i}{m_e 4\pi}}\exp\left(-\phi/T_e\right)\right]
\end{aligned}
$$

$$
\omega = \nabla\cdot\left(\frac{n}{B^2}\nabla_\perp\phi\right)
$$